Heat and Mass Transfer Investigation of Oldroyd-B Fluid in a Curved Symmetric Channel

P. Praveen Kumar[1,2*], S. Balakrishnan[1], P. Tamizharasi[3], A. Magesh[4]

[1]Department of Mathematics, Islamiah College,Vaniyambadi, Tamilnadu, India 635 752, (Affilated to Thiruvalluvar University, Serkkadu, Vellore, Tamilnadu, India 632 115)
[2]Department of Mathematics, Sathya College of Arts and Science, Ranipet, Tamilnadu, India 632 509 (Affilated to Thiruvalluvar University, Serkkadu, Vellore, Tamilnadu, India 632 115)
[3]Department of Mathematics, Easwari Engineering College Chennai, Tamilnadu, India. 600 089.
[4]Department of Mathematics, Sri Sai Ram Engineering College, Chennai, Tamilnadu, India 600 044.
Email: ppk.kandha@gmail.com
*Corresponding Author

Received: 17.04.2024 Revised : 11.05.2024 Accepted: 15.05.2024

ABSTRACT
This study analyzed themass/heat transfer of the Oldroyd-B liquid model by peristaltic mechanism in the appearence of an electrically conductive magnetic parameter through a curved channel. The governing equation of the Oldroyd-B liquid model is formulated and lengthy equations are shortened by the considerations of long wavelengths and very small Reynolds number approximations. The exact results were calculated. The impact of various fluid parameters influid's velocity, concentration, temperature, Sherwood number, and Nusselt number are illustrated through the computational mathematical software Matlab, and the stream function is computed through Mathematica. The impact of important parameters of the relevant fluids was discussed.

Keywords: Peristaltic flow, Oldroyd-B fluid, Curved channel, Magnetic field

1. INTRODUCTION

Peristaltic motion is a phenomenon where fluid motion occurs when a progressive wave of expansion or contraction of the area extends along the distensible tube or channel. This mechanism is widely used in biomedical, engineering, and other industries. Some of the applications in industries are plastics manufacturing, locomotion of worms, toxic liquid movement in the nuclear industry, ketchup, food processing, the performance of lubricants, sanitary fluid transportation, finger and roller pumps. In physiology, in the vasomotion of venules, urine movement to bladder from kidney, capillaries, and arterioles, swallowing food via the esophagus, etc.Latham [1] started the peristaltic flow of fluid motion in two-dimensional Cartesian coordinates in his thesis. Burns and Parkes [2], Shapiro et al. [3] both expand on this study. To simplify the governing equations, they used long wavelength and small Reynolds number assumptions. Asymmetric channels with Newtonian fluid were examined by Mishra and Rao [4]. The magnetic field of the peristaltic mechanism plays a major role in bio-engineering and medicine. Some of the applications are in the development of magnetic tracers, bleeding reductions during surgeries, drug transport, hyperthermia, magnetic devices built for cell separation, etc. Heat transfer of fluid transport through peristalsis works in numerous applications in oxygenation, food processing, tissue conduction, hemodialysis, and radiation between the environment and its surroundings. Concentration (Mass) transfer involves important applications in the diffusion of chemical impurities, separation membrane and process of combustion, the study of warm salty springs in the ocean, etc. Some of the investigations based on the peristaltic transport of various liquid models with mass/heat transfer under the involvement of various body forces in different geometries are presented [5-23].Nevertheless, the majority of the previously described research on peristalsis use flat or straight channels, which may not be sufficient when considering flows through glandular and physiological conduits. We encounter curved geometries in physical and industrial processes, where curvilinear coordinates must be taken into account in order to counter challenging mathematical statements. Sato et al. [24] initially explored the peristaltic motion of liquid particles in two-dimensional Cartesian coordinates through the curved channel. Some studies of related to curved channel presented in [25-40].

The present study aims to construct upon the investigations to analyze mass/heat transfer of Oldroyd-B fluid with a magnetic field under peristalsis. We have tried to construct a mathematical formulation to

provide a realistic manifestation of the blood flow. So, the fluid motion is taken into account in curved channels because many of the glandular ducts and arteries are curved. No investigations have been discussed yet by considering the Oldroyd-B fluid model with mass/heat transfer investigations under the impact of the magnetic field. Therefore, the relevant mathematical formulation is made based onthe flow pattern and the equations are abridged with the help of lubrication theory approximation. Reduced equations of the velocity, energy and mass transfer equations are exactly solved. The results are discussed for various values of involved pertinent parameters through the graphs.

2. Mathematical structure

A2-dimensionalincompressible Oldroyd-Bliquid in a curved geometry with uniform half-width a, center O, and radius Υ. The deformable channel walls are propagated by sinusoidal waves with velocity c See Figure 1.

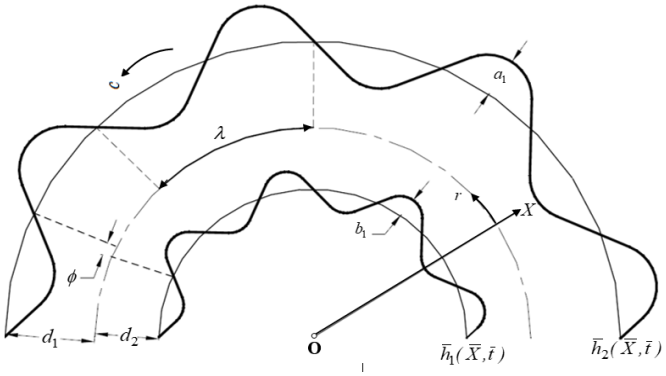

Figure 1. Flow geometry of the curved channel.

The shape of the wave is represented as [24]

$$\bar{h}_1 = -a - b\sin\left[\frac{2\pi}{\lambda}\left(x - c\bar{t}\right)\right]$$
$$\bar{h}_2 = a + b\sin\left[\frac{2\pi}{\lambda}\left(x - c\bar{t}\right)\right] \quad (1)$$

where λ, t, b are the wavelength, time, wave amplitude.

In the radial direction, the fluid particle is electrically conducting withan externally applied magnetic field B.

$$B = \left(\frac{B_0}{r+\Upsilon}, 0, 0\right) \quad (2)$$

In which B_0 isthe magnetic field strength, Ohm's law yields the subsequent expression.

$$J \times B = \left(0, -\frac{\sigma B_0^2 U}{(r+\Upsilon)^2}, 0\right) \quad (3)$$

Where J, σ are current density, electrical conductivity.

The constitutive equations for the Oldroyd-B fluid model are given by[37]

$$\tau = -pI + S \quad (4)$$

$$\left(1 + \lambda_2 \frac{d}{dt}\right) S = \mu\left(1 + \lambda_2 \frac{d}{dt}\right) A_1, \quad (5)$$

$$A_1 = L + L^T, L = \text{grad } V$$

The component of the extra tense tensorScan be described as follows:

$$\left(1+\lambda_1\left(\frac{\partial}{\partial t}+\frac{\Upsilon u}{r+\Upsilon}\frac{\partial}{\partial x}+v\frac{\partial}{\partial r}\right)\right)S_{rr}=2\mu\left(1+\lambda_2\left(\frac{\partial}{\partial t}+\frac{\Upsilon u}{r+\Upsilon}\frac{\partial}{\partial x}+v\frac{\partial}{\partial r}\right)\right)\frac{\partial v}{\partial r},$$

$$\left(1+\lambda_1\left(\frac{\partial}{\partial t}+\frac{\Upsilon u}{r+\Upsilon}\frac{\partial}{\partial x}+v\frac{\partial}{\partial r}\right)\right)S_{xr}=\mu\left(1+\lambda_2\left(\frac{\partial}{\partial t}+\frac{\Upsilon u}{r+\Upsilon}\frac{\partial}{\partial x}+v\frac{\partial}{\partial r}\right)\right)\left(\frac{\partial u}{\partial r}+\frac{\Upsilon u}{r+\Upsilon}\frac{\partial v}{\partial x}-\frac{u}{r+\Upsilon}\right),$$

$$\left(1+\lambda_1\left(\frac{\partial}{\partial t}+\frac{\Upsilon u}{r+\Upsilon}\frac{\partial}{\partial x}+v\frac{\partial}{\partial r}\right)\right)S_{xx}=2\mu\left(1+\lambda_2\left(\frac{\partial}{\partial t}+\frac{\Upsilon u}{r+\Upsilon}\frac{\partial}{\partial x}+v\frac{\partial}{\partial r}\right)\right)\left(\frac{\Upsilon}{r+\Upsilon}\frac{\partial u}{\partial x}+\frac{v}{r+\Upsilon}\right),$$

where I , τ, μ, p , λ_1, λ_2 , S are the Identity tensor,Cauchy stress tensor, dynamic viscosity, pressure, relaxation and the retardation times, extra stress tensor, and A_1 is a first Rivlin Ericksen tensor. Theequations governingfor an Oldroyd-B fluid model is defined as

$$\frac{\partial v}{\partial r}+\frac{\Upsilon}{\Upsilon+\mathrm{r}}\frac{\partial u}{\partial x}+\frac{v}{\Upsilon+\mathrm{r}}=0 \tag{6}$$

$$\rho\left(\frac{\partial v}{\partial t}+v\frac{\partial v}{\partial r}+\frac{\Upsilon u}{\Upsilon+\mathrm{r}}\frac{\partial v}{\partial x}-\frac{u^2}{r+\Upsilon}\right)=-\frac{\partial P}{\partial r}+\frac{\mu}{r+\Upsilon}\frac{\partial S_{rr}}{\partial r}+\frac{\mu\Upsilon}{r+\Upsilon}\frac{\partial S_{xr}}{\partial x}-\frac{\mu S_{xx}}{r+\Upsilon} \tag{7}$$

$$\rho\left(\frac{\partial u}{\partial t}+v\frac{\partial u}{\partial r}+\frac{\Upsilon u}{\Upsilon+\mathrm{r}}\frac{\partial u}{\partial x}-\frac{uv}{r+\Upsilon}\right)=-\frac{\Upsilon}{r+\Upsilon}\frac{\partial P}{\partial x}+\mu\frac{\partial S_{rx}}{\partial r}+\frac{\mu\Upsilon}{r+\Upsilon}\frac{\partial S_{xx}}{\partial x}-\frac{\sigma B_0^2 u}{(r+\Upsilon)^2} \tag{8}$$

$$\rho c_p\left(\frac{\partial T}{\partial t}+v\frac{\partial T}{\partial r}+\frac{\Upsilon u}{\Upsilon+\mathrm{r}}\frac{\partial T}{\partial x}\right)=\kappa_t\left(\frac{\partial^2 T}{\partial r^2}+\frac{1}{r+\Upsilon}\frac{\partial T}{\partial r}+\left(\frac{\Upsilon}{r+\Upsilon}\right)\frac{\partial^2 T}{\partial x^2}\right)$$
$$+\frac{Dk_t}{C_s}\left(\frac{\partial^2 C}{\partial r^2}+\frac{1}{r+\Upsilon}\frac{\partial C}{\partial r}+\left(\frac{\Upsilon}{r+\Upsilon}\right)\frac{\partial^2 C}{\partial x^2}\right)+tr\left(LS\right) \tag{9}$$

$$\left(\frac{\partial C}{\partial t}+v\frac{\partial C}{\partial r}+\frac{\Upsilon u}{\Upsilon+\mathrm{r}}\frac{\partial C}{\partial x}\right)=D\left(\frac{\partial^2 C}{\partial r^2}+\frac{1}{\Upsilon+\mathrm{r}}\frac{\partial C}{\partial r}+\left(\frac{\Upsilon}{\Upsilon+\mathrm{r}}\right)\frac{\partial^2 C}{\partial x^2}\right)$$
$$+\frac{Dk_t}{T_m}\left(\frac{\partial^2 T}{\partial r^2}+\frac{1}{r+\Upsilon}\frac{\partial T}{\partial r}+\left(\frac{\Upsilon}{r+\Upsilon}\right)\frac{\partial^2 T}{\partial x^2}\right). \tag{10}$$

Here ρ, υ, T, C are the density, kinematic viscosity, temperature, concentration, c_p, C_s, T_m, κ_t , D, k_t are the specific heat, concentration susceptibility,mean fluid temperature,thermal conductivity, mass diffusivity coefficient, thermal diffusion ratio. Here $L=\operatorname{grad} V$. In the fixed frame (r, x) the fluid velocity is not steady. For steady flow analysis, the fixed frame is transformed into the wave frame $(\bar{r}, \bar{x})$ using the Galilean transformations [40].

$$\bar{r}=r, \bar{x}=x-ct, \bar{v}=v, \bar{u}=u-c \tag{11}$$

We Introducing the following dimensionless quantities are

$$\eta=\frac{\bar{r}}{a}, v^*=\frac{\bar{v}}{c}, p^*=\frac{a^2}{\mu\lambda c}\bar{p}, \delta=\frac{a}{\lambda}, S_{ij}{}^*=\frac{aS_{ij}}{c\mu}, \psi^*=\frac{\psi}{ca}, x^*=\frac{\bar{x}}{\lambda}, u^*=\frac{\bar{u}}{c},$$

$$E=\frac{c^2}{T_0 c_p}, k=\frac{\Upsilon}{a}, H^2=\frac{\sigma B_0^2}{\mu}, Sr=\frac{\rho D\kappa_t T_0}{\mu T_m C_0}, Du=\frac{D\kappa_t C_0}{\mu C_s C_p T_0}, \mathrm{Pr}=\frac{\mu C_0}{\kappa_t}, \varphi=\frac{C-C_0}{C_0},$$

$$Br=E\,\mathrm{Pr}, Sc=\frac{\mu}{\rho D}, \theta=\frac{T-T_0}{T_0}, Br=\frac{\mu c^2}{\kappa\left(T_0-T_1\right)}, \mathrm{Re}=\frac{\rho ca}{\mu} \tag{12}$$

And the dimensionless stream function

$$u=-\frac{\partial\psi}{\partial\eta}, v=\delta\frac{k}{\eta+k}\frac{\partial\psi}{\partial s} \tag{13}$$

Applying Eq. (11) into Eqs. (6)-(10) and then with the help of Eqs. (12) and (13),consideration oftiny Reynolds number, long wavelength,Eq. (6) is satisfied and Eqs. (7)– (10) after removing (*) becomes

$$\frac{\partial p}{\partial \eta}=0, \tag{14}$$

$$-\frac{k}{\eta+k}\frac{\partial p}{\partial x}+\frac{1}{(\eta+k)^2}\frac{\partial}{\partial \eta}\left((\eta+k)^2 S_{rx}\right)+\frac{\left(\psi_\eta-1\right)H^2}{(\eta+k)^2}=0, \tag{15}$$

$$\frac{\partial^2\theta}{\partial\eta^2}+\frac{1}{\eta+k}\frac{\partial\theta}{\partial\eta}+\Pr Du\left(\frac{\partial^2\varphi}{\partial\eta^2}+\frac{1}{\eta+k}\frac{\partial\varphi}{\partial\eta}\right)+Br\left(-\psi_{\eta\eta}+\frac{\psi_\eta}{\eta+k}-\frac{1}{r+k}\right)S_{xr}=0, \tag{16}$$

$$\frac{1}{Sc}\left(\frac{\partial^2\varphi}{\partial\eta^2}+\frac{1}{\eta+k}\frac{\partial\varphi}{\partial\eta}\right)+Sr\left(\frac{\partial^2\theta}{\partial\eta^2}+\frac{1}{\eta+k}\frac{\partial\theta}{\partial\eta}\right)=0, \tag{17}$$

In above expressions, $Re,\delta,E,Br,Sc,Sr,Du,Pr,H$ are Reynolds number, wave number, Eckert number,Brinkmann number, Schimdt number,Soret number,Dufour number Prandtl number, Hartmann number.

Eq. (14) shows the pressure is not dependent of η.

$$\frac{\partial}{\partial\eta}\left[\frac{1}{\left(\eta+k\right)k}\frac{\partial}{\partial\eta}\left((k+\eta)^2 S_{rx}\right)+\frac{H^2\left(\psi_\eta-1\right)}{k\left(\eta+k\right)}\right]=0, \tag{18}$$

Where $S_{rx}=S_{xr}=\left(-\psi_{\eta\eta}+\frac{\psi_\eta}{\eta+k}-\frac{1}{\eta+k}\right)$, (19)

The correspondingboundariesare

$$\psi=-\frac{F}{2},\quad \frac{\partial\psi}{\partial\eta}=-1,\theta=0,\varphi=0 \ at\ h_1=-1-\varepsilon\sin(x),$$

$$\psi=\frac{F}{2},\frac{\partial\psi}{\partial\eta}=-1,\theta=1,\varphi=1 \ at\ h_2=1+\varepsilon\sin x, \tag{20}$$

In the fixed frame the volume flow rate in the dimensional form as [26]

$$Q=\int_{\bar{h}_1}^{\bar{h}_2}\bar{U}\,d\bar{R} \tag{21}$$

here $\bar{h}_2$ and $\bar{h}_1$ are functions of $\bar{t}$ and x. The wave frame is as follows

$$q=\int_{\bar{h}_1}^{\bar{h}_2}\bar{u}\,dr \tag{22}$$

where $\bar{h}_2$ and $\bar{h}_1$ are functions of $\bar{x}$ alone. Eqs (21) and (22) can be presented as

$$Q=ch_2-ch_1+q \tag{23}$$

the average volume flow rate $\left(T=\lambda/c\right)$ is

$$\overline{Q}=\frac{1}{T}\int_0^T Q dt=\frac{1}{T}\int_0^T\left(ch_2-ch_1+F\right)dt=q+2ac, \tag{24}$$

the mean flow Θ in the fixed frame and q in the wave frame is defined as

$$\Theta=\frac{\overline{Q}}{ac},F=\frac{q}{ac} \tag{25}$$

Therefore, applyingeq. (25)into eq. (24) we get

$$\Theta=F+2 \tag{26}$$

3. Solution of the problem

The solution of Eqs.(18), (16) and (17) with Eq.(20) we get.

$$\psi = c_1 \frac{(\eta+k)^{1+\sqrt{1+H^2}}}{1+\sqrt{1+H^2}} + c_2 \frac{(\eta+k)^{1-\sqrt{1+H^2}}}{1-\sqrt{1+H^2}} + c_3\left(2k\eta+\eta^2\right) + c_4 + \frac{\eta+k}{1+H^2} \quad (27)$$

$$\theta = c_{11}\log(\eta+k) + c_{12} + \frac{Br}{(1+H^2)^2\left(-1+\Pr DuScSr\right)}$$

$$\left[\left(l_1^2+2H^2l_1\right)\frac{(\eta+k)^{\sqrt{1+H^2}}}{1+H^2} + \left(l_2^2+H^2l_2\right)\frac{(\eta+k)^{-\sqrt{1+H^2}}}{1+H^2} + \frac{2l_1l_2}{\eta+k} + \frac{H^4\log(\eta+k)^2}{2}\right]$$

(28)

$$\varphi = c_{21}\log(\eta+k) + c_{22} - \frac{BrScSr}{(1+H^2)^2\left(-1+\Pr DuScSr\right)}$$

$$\left[\left(l_1^2+2H^2l_1\right)\frac{(\eta+k)^{\sqrt{1+H^2}}}{1+H^2} + \left(l_2^2+H^2l_2\right)\frac{(\eta+k)^{-\sqrt{1+H^2}}}{1+H^2} + \frac{2l_1l_2}{\eta+k} + \frac{H^4\log(\eta+k)^2}{2}\right] \quad (29)$$

Where constants appeared in the above equations arelengthy expressions. So, it is given in the appendix.

The z and Sh for both the walls are defined as[7]

$$z = \frac{\partial h_i}{\partial x}\left(\frac{\partial\theta}{\partial\eta}\right)_{\eta=h_i}, i=1,2 \text{ (heat transfer coefficient)} \quad (30)$$

$$Sh = \frac{\partial h_i}{\partial x}\left(\frac{\partial\varphi}{\partial\eta}\right)_{\eta=h_i}, i=1,2 \text{ (Sherwood number)} \quad (31)$$

4. RESULT AND DISCUSSION

In this part, variations of velocity, φ, θ, z, Sh and streamlines are examined for the different values of the involved parameter.

4.1. Velocity distribution

Velocity distributions are presented in Fig.2(a) and (b). The result of the variations of velocity for the curvature parameter is presented in Fig.2(a).

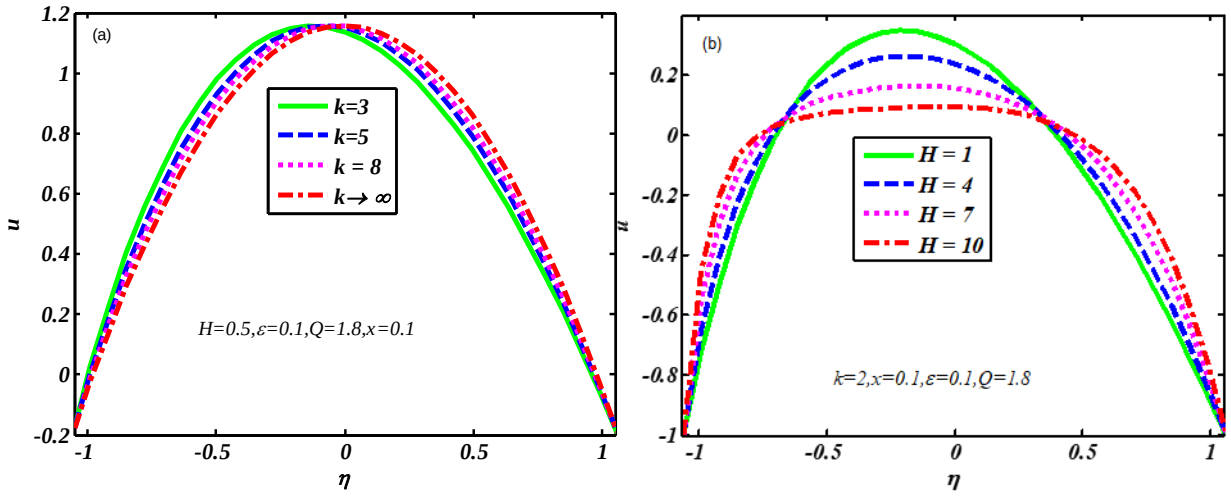

Figure 2. Velocity Distribution

This graph indicates, the velocity profile seems asymmetric in the curved channel,for a larger k the velocity profile is symmetric. Fig.2(b), presented for velocity variation of H .This figure shows, the velocity of the liquid reduces fora large value of H . Actually, Lorentz force produce resistance in the fluid flow field. Furthermore, increasing the magnetic field strength provides an obstruction for the high-pressure gradient to travel inside the curved channel. Consequently, the magnetic field seems to be a delaying factor in the radial direction for fluid movement. Magnetic fields have an inverse behaviour and are beneficial in the treatment of disorders such as migraine headaches, joint difficulties, depression, cancer, etc.

4.2. Temperature and concentration distribution

In this subsection, we have analyzed the temperature distribution for involved fluid parameters like curvature parameter k , Brinkman number Br and H . The concluded results of
Fig. 3(a)

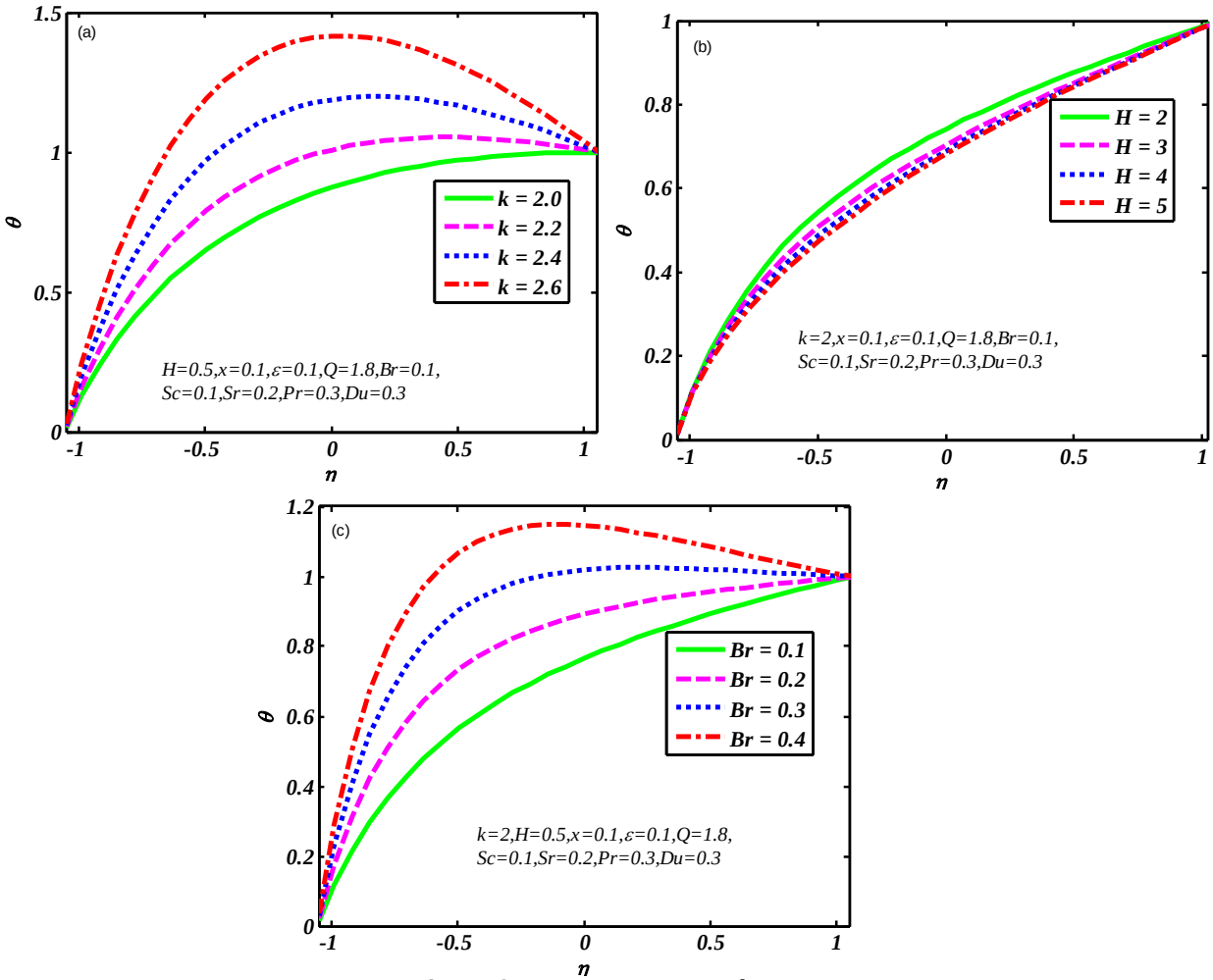

Figure 3. Temperature Distribution

manifest raises the temperature towards straight channel.The temperature of the liquid diminishes for the magnetic parameter boosts see Fig. 3(b). This could be due to the flow being affected by the ohmic heating of the magnetic field. Moreover, a strong magnetic field is produced for larger H, which cools the fluid by removing heat and generating current in the motors. Fig. 3(c). The temperature profile went up to large Brinkman number (Br) values. Taking into account that the Br suggests effects on viscous dissipation that cause heat to be produced inside the channel.

Fig.4. (a-e) plotted for concentration profiles against the pertinent involved dimensionless parameters. From the above mentioned Figures, we noticed that reduction behavior of (ϕ) concentration concluded

towards curvature parameter k see Fig.4(a), Hartmann number H Fig.4(b) and Brinkmann number Br Fig.4(c).

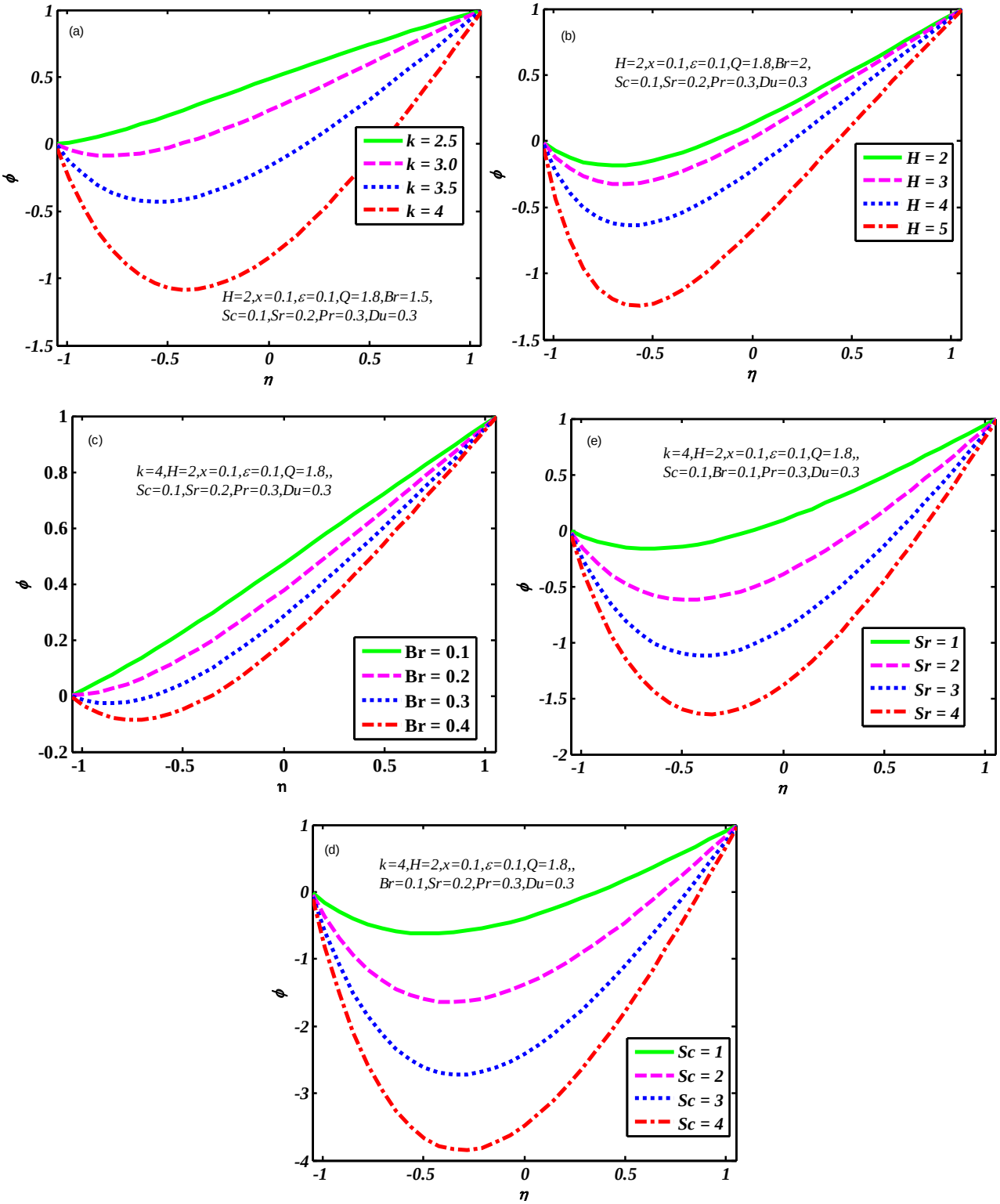

Figure 4. Concentration Distribution

Schmidt number Sc is the ratio between momentum and mass diffusivity. Therefore, it is perceivable from Fig. 4(d) that concentration reduces as Sc boosted. Similar trend concluded for greater Sr values see Fig.4(e).

4.3. Heat transfer coefficient and Sherwood number

Fig. 5. (a-c) presented for the behavior of heat transfer coefficient against k, H, Br, Sc and Sr From this diagram, we clarify that due to the peristaltic mechanism, the coefficient of thermal transfer profile is oscillatory behavior.

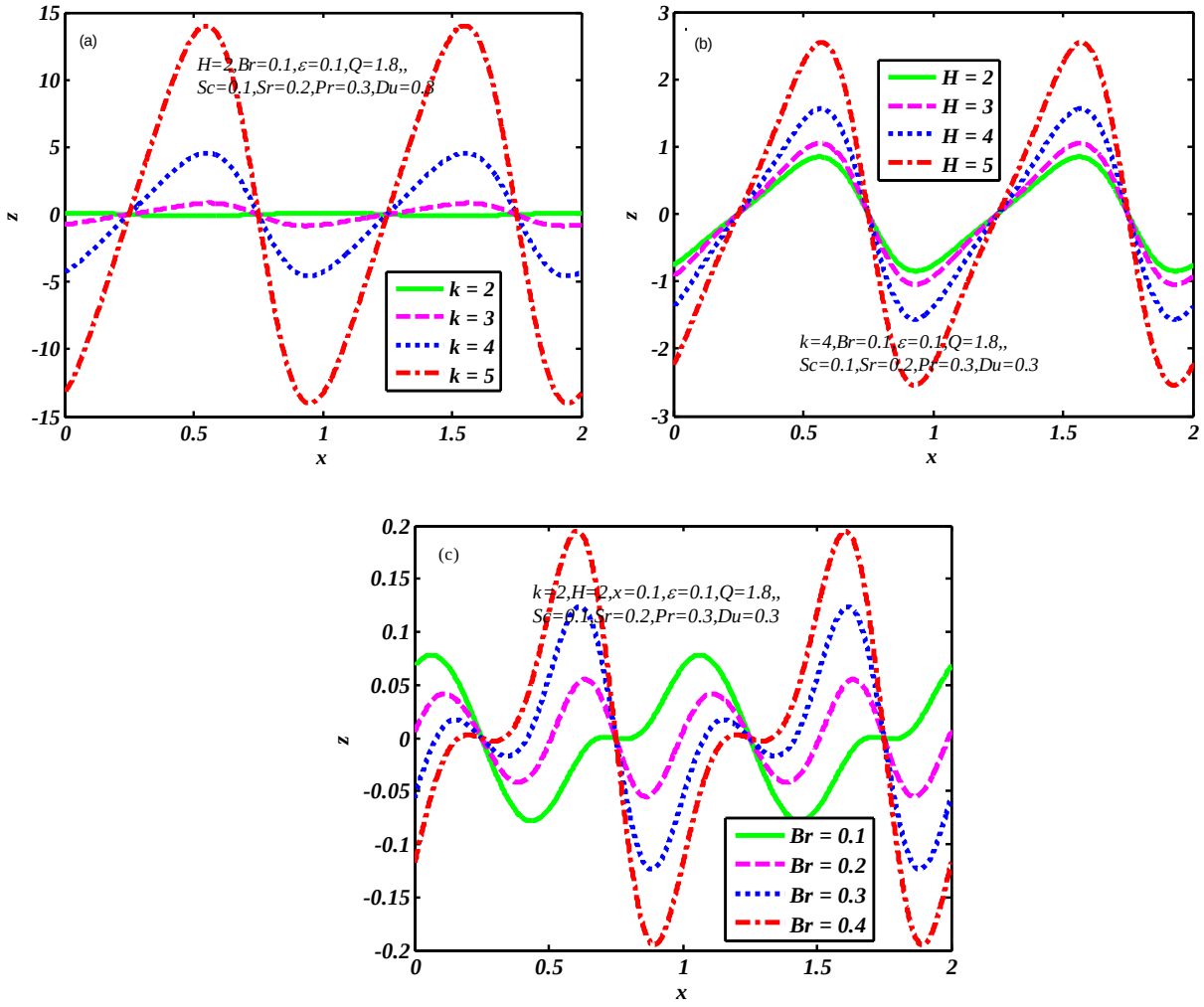

Figure 5. Variation of Heat Transfer Co-efficient z

The magnitude of heat transfer h_x coefficient increases in the region $(0.25 < x < 0.75)$ and $(1.25 < x < 1.75)$ decreases in the region $(0.75 < x < 1.25)$. Similar behavior of h_x concluding for Sherwood number. ie., oscillatory behavior. But increasing values of k, H, Br, Sc and Sr the Sherwood number reduces in the region $(0.25 < x < 0.75)$ and $(1.25 < x < 1.75)$ raises in the region $(0.75 < x < 1.25)$ see the Figs.6.(a-e).

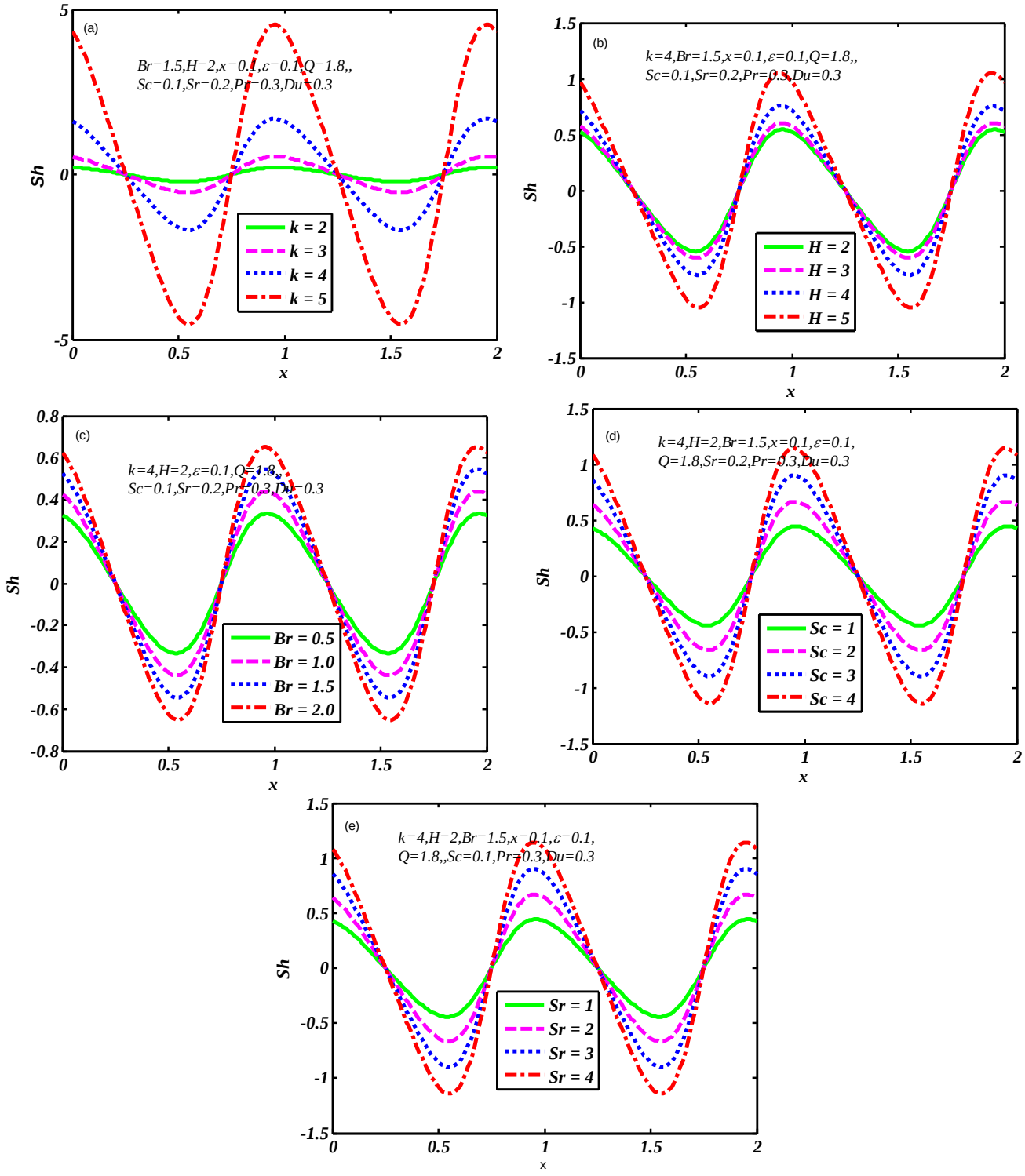

Figure 6. Sherwood Number Variation

4.4. Trapping Results

The trapping pattern is another important mechanism to analyze the flow of fluid. Peristaltic transport can be investigated by examining a closed contour of streamlines at various wave amplitudes and average time flow rates. The process is known as trapping. From a physiological standpoint, fluids might become trapped as a result of continuous smooth border movements, which is good for adequately propelling the biological working fluid from one location to another. With the proper extension, the working organs can be kept alive for an extended period of time without complications. Therefore, trapping phenomena can be studied by displaying the stream functions relative to k and H. Fig. 7. (a-d) presented for streamlines

for k variation. It is concluded that the dimensions of the trapped bolus decrease in the upper peristaltic wall, also increase in the lower wall at high curvature, with the bolus disappearing in the upper wall to the curved to straight channel. Fig. 8. (a-d) depicts the size of the trapped bolus in the upper wall increases at the same time the lower wall decreases with the increasing amount of H.

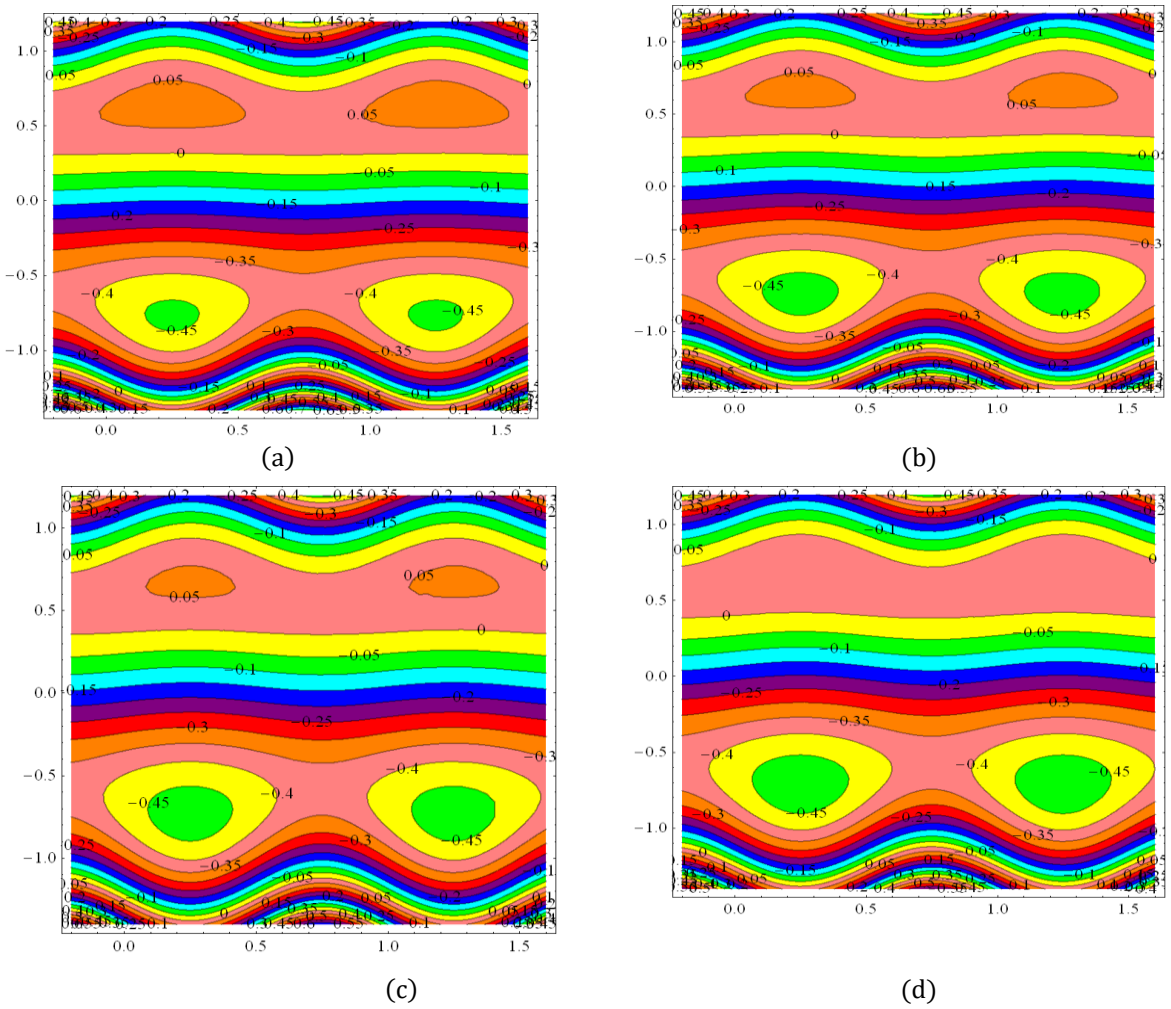

(a) (b)

(c) (d)

Figure 7. Streamlines for $(a)k=2,(b)k=4(c)k=6,(d)k=8$ the other parameters are $x=0.1,Q=1.8,H=2,\varepsilon=0.1$

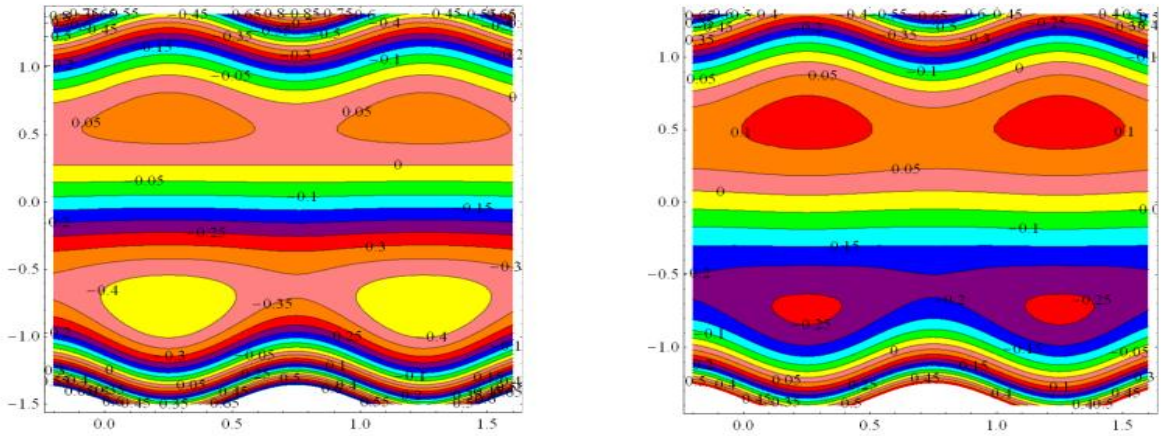

(a) (b)

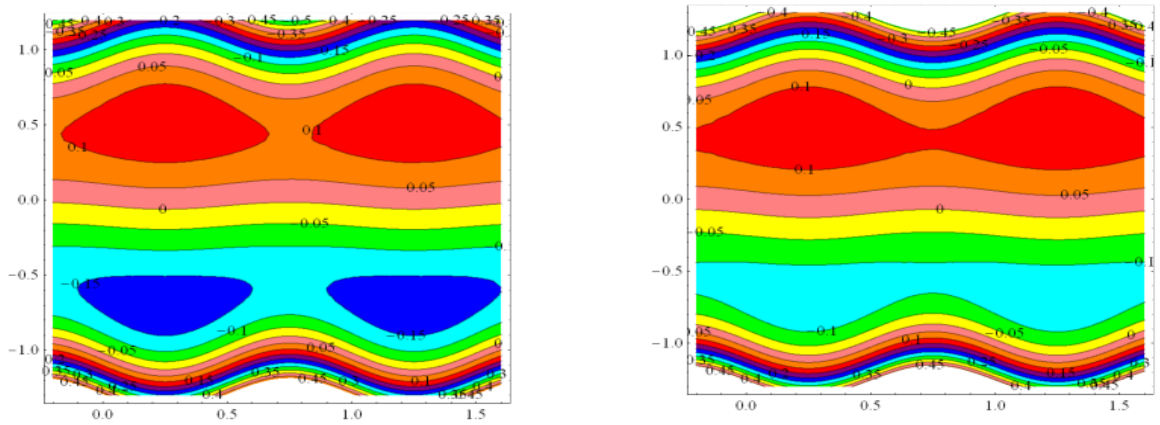

(c) (d)

Figure 8. Streamlines for $(a)H=2,(b)H=3(c)H=4,(d)H=5$ the other parameters are $x=0.1,Q=1.8,k=3,\varepsilon=0.1$

5. CONCLUSION

In this paper we analyzed the mass and energy transfer of the Oldroyd-B liquid through a symmetrical curved channel under peristaltic mechanism. The key findings are presented below

1. Parabolic nature concluded in the velocity profile and also symmetric in the planner channel, but non-symmetric in the curved channel.
2. Reduces the velocity towards the massive quantity of H
3. The enhanced amount of k,H,Br temperature raises, but concentration reduces. The same reduction concluded for raising the values of Sc,Sr
4. $h_{x,}Sh$ Profiles are oscillatory behavior concluded. h_x Increases but Sh decreases in the upper walls for small to large values k,H,Br and k,H,Br,Sc,Sr respectively.
5. Bolus size and number of streamlines lowered for the straight channel, but raises for H increases.

Appendix`

$$\alpha_2=1-\sqrt{1+H^2}\,,\alpha_1=1+\sqrt{1+H^2}\,,\alpha_3=(h_2+k)(h_1+k)^{\alpha_1-1}-(h_1+k)(h_2+k)^{\alpha_1-1},$$

$$\alpha_4=(h_2+k)(h_1+k)^{\alpha_2-1}-(h_1+k)(h_2+k)^{\alpha_2-1},\qquad \alpha_5=\frac{(h_2+k)^{\alpha_1}-(h_1+k)^{\alpha_1}}{\alpha_1},$$

$$\alpha_6=\frac{(h_2+k)^{\alpha_2}-(h_1+k)^{\alpha_2}}{\alpha_2},\qquad \alpha_7=(h_2-h_1)\left(k+\frac{h_2+h_1}{2}\right),\qquad \alpha_8=F(h_1+k)+\alpha_7,$$

$$\alpha_9=\alpha_5(h_1+k)-\alpha_7(h_1+k)^{\alpha_1-1},\qquad \alpha_{10}=\alpha_6(h_1+k)-\alpha_7(h_1+k)^{\alpha_2-1},$$

$$c_1=\frac{1}{\alpha_1}\frac{\alpha_{10}(h_1-h_2)-\alpha_4\alpha_8}{\alpha_3\alpha_{10}-\alpha_4\alpha_9}=\alpha_{11},c_2=\frac{1}{\alpha_2}\frac{\alpha_8-\alpha_9\alpha_{11}}{\alpha_{10}}=\alpha_{12},\ c_3=\frac{1}{\alpha_3}\frac{F-\alpha_5\alpha_{11}-\alpha_6\alpha_{12}}{\alpha_{17}},$$

$$c_4=\frac{F}{2}-\left(\frac{c_1(h_2+k)^{\alpha_1}}{\alpha_1}+\frac{c_2(h_2+k)^{\alpha_2}}{\alpha_2}+c_3\left(h_2k+\frac{h_2^2}{2}\right)\right),$$

$$l_1=c_1(\alpha_1-2)(1+H^2),$$

$$l_2=c_2(\alpha_2-2)(1+H^2)$$

$$C_{11}=\frac{1-\dfrac{Br}{\left(1+H^2\right)^2\left(-1+Pr\,DuScSr\right)}\left\{\begin{array}{l}\dfrac{\left(2H^2l_1+l_1^2\right)}{1+H^2}\left[\left(h_2+k\right)^{\sqrt{1+H^2}}-\left(h_1+k\right)^{\sqrt{1+H^2}}\right]+\dfrac{\left(2H^2l_2+l_2^2\right)}{1+H^2}\\ \left[\left(h_2+k\right)^{-\sqrt{1+H^2}}-\left(h_1+k\right)^{-\sqrt{1+H^2}}\right]+\dfrac{H^4}{2}\left[log\left(h_2+k\right)^2-log\left(h_1+k\right)^2\right]+2l_1l_2\dfrac{\left(h_1-h_2\right)}{\left(h_2+k\right)\left(h_1+k\right)}\end{array}\right\}}{log\left(h_2+k\right)-log\left(h_1+k\right)}$$

$$c_{12}=1-\left\{c_{11}\,log\left(h_2+k\right)+\frac{Br}{\left(1+H^2\right)^2\left(-1+Pr\,DuScSr\right)}\left[\left(l_1^2+2H^2l_1\right)\frac{\left(h_2+k\right)^{\sqrt{1+H^2}}}{1+H^2}+\left(l_2^2+H^2l_2\right)\frac{\left(h_2+k\right)^{-\sqrt{1+H^2}}}{1+H^2}+\frac{2l_1l_2}{h_2+k}+\frac{H^4\,log\left(h_2+k\right)^2}{2}\right]\right\}$$

$$C_{21}=\frac{1-\dfrac{BrScSr}{\left(1+H^2\right)^2\left(-1+Pr\,DuScSr\right)}\left\{\begin{array}{l}\dfrac{\left(2H^2l_1+l_1^2\right)}{1+H^2}\left[\left(h_2+k\right)^{\sqrt{1+H^2}}-\left(h_1+k\right)^{\sqrt{1+H^2}}\right]+\dfrac{\left(2H^2l_2+l_2^2\right)}{1+H^2}\\ \left[\left(h_2+k\right)^{-\sqrt{1+H^2}}-\left(h_1+k\right)^{-\sqrt{1+H^2}}\right]+\dfrac{H^4}{2}\left[log\left(h_2+k\right)^2-log\left(h_1+k\right)^2\right]+2l_1l_2\dfrac{\left(h_1-h_2\right)}{\left(h_2+k\right)\left(h_1+k\right)}\end{array}\right\}}{log\left(h_2+k\right)-log\left(h_1+k\right)}$$

$$c_{22}=1-\left\{c_{11}\,log\left(h_2+k\right)+\frac{BrScSr}{\left(1+H^2\right)^2\left(-1+Pr\,DuScSr\right)}\left[\begin{array}{l}\left(l_1^2+2H^2l_1\right)\dfrac{\left(h_2+k\right)^{\sqrt{1+H^2}}}{1+H^2}+\left(l_2^2+H^2l_2\right)\dfrac{\left(h_2+k\right)^{-\sqrt{1+H^2}}}{1+H^2}\\ +\dfrac{2l_1l_2}{h_2+k}+\dfrac{H^4\,log\left(h_2+k\right)^2}{2}\end{array}\right]\right\}$$

REFERENCES

[1] T.W. Latham, Fluid motion in a peristaltic pump MS Thesis, MIT Cambridge, 1969.

[2] J.C. Burns, T. Parkes, Peristaltic motion, J. Fluid. Mech. 29 (1967) 731-743.

[3] A.H. Shapiro, M.Y. Jaffrin, S.L. Weinberg, Peristaltic pumping with long wavelengths at low Reynolds number, J. Fluid. Mech.37 (1968) 799-825.

[4] M. Mishra, A. Ramachandra Rao, Peristaltic transport of a Newtonian fluid in an asymmetric channel, Z. Ange. Math. Phys. 54 (2003) 532-550.

[5] K. Vajravelu, S. Sreenadh, V. Ramesh Babu, Peristaltic transport of a Herschel Bulkley fluid in an inclined tube, Int. J. Non-Linear. Mech. 40 (2005) 83-90.

[6] A. Madani, D.M. Martinez, J.A. Olson, Ian Frigaard, The stability of spiral Poiseuille flows of Newtonian and Bingham fluids in an annular gap, J. Non-Newton. Fluid. Mech. 193 (2013) 3-10.

[7] Y. Wang, T. Hayat, N. Ali, M. Oberlack, Magnetohydrodynamic peristaltic motion of a Sisko fluid in a symmetric or asymmetric channel, Physica A. 387 (2008) 347–362.

[8] S. Mekheimer Kh, S.Z.A. Husseny, Y. Abd Elmaboud, Effects of heat transfer and space porosity on peristaltic flow in a vertical asymmetric channel, Numer. Methods for Partial. Diff. Eqs. 26 (2010)747-770.

[9] S. Nadeem, S. Akram, Influence of inclined magnetic field on peristaltic flow of a Williamson fluid model in an inclined symmetric or asymmetric channel, Math. Comp. Mod. 52 (2010) 107-119.

[10] A. Magesh, P. Praveen Kumar, P. Tamizharasi, R. Vijayaragavan, S. Vimal Kumar, M. Kothandapani, Effect of magnetic field on the peristaltic transport of Oldroyd-B fluid in an asymmetric inclined channel, J Phy: Conf Ser 1850 (2021) 012111.

[11] P. Praveen Kumar, S. Balakrishnan, A. Magesh, Peristaltic Transport of (Al2O3/H2O) Nanofluid through A Vertical Asymmetric Channel with MHD Effects, J. Prop. Tech.44 (2023) 1198-1207.

[12] P. Praveen Kumar, S. Balakrishnan, A. Magesh, P. Tamizharasi, S.I Abdelsalam, Numerical treatment of entropy generation and Bejan number into an electroosmotically-driven flow of Sutterby nanofluid in an asymmetric microchannel, Numer. Heat. Tr. B-Fund.(2024) 1-20.

[13] Z. Abbas, M. Naveed, M. Sajid, Hydromagnetic slip Flow of nano fluid over curved stretching surface with heat generation and thermal radiation, J. Mol. Liq. 215 (2016) 756 – 762.

[14] S. Nadeem, A. Riaz, R. Ellahi, N.S. Akbar, Mathematical model for the peristaltic flow of Jeffrey fluid with nano particles phenomenon through a rectangular duct, Appl. Nano. Sci. 4 (2014) 613-624.

[15] M.V. Subba Reddy, A. Ramachandra Rao, S. Sreenath, Peristaltic motion of a power-law fluid in an asymmetric channel, Int. J. Non-linear. Mech. 42 (2007) 1153-1161.

[16] S.I. Abdelsalam, M.M. Bhatti, The study of non-Newtonian nanofluid with hall and ion slip effects of peristaltically induced motion in a non-uniform channel, RSC. Adv. 8 (2018) 7904–7915.

[17] M. Moyers-Gonzalez, Ian Frigaard, Dean flow of a Bingham fluid in a curved rectangular duct, J. Non-Newton. Fluid. Mech.286 (2020) 104440.
[18] S. Srinivas, V. Pushparaj, Non-linear peristaltic transport in an inclined asymmetric channel, Commun. Nonlinear Sci. Numer. Simul. 13 (2008) 1782-1795.
[19] S. Nadeem, S. Noreen, M.Y. Malik, Numerical solutions of peristaltic flow of a Newtonian fluid under the effects of magnetic field and heat transfer in a porous concentric tube. Z. Naturforsch. 65 (2010) 369–380.
[20] A. Magesh, M. Kotandapani, V. Pushparaj, Electro-Osmotic flow of Jeffry fluid in an asymmetric micro channel under the effect of magnetic field, J Phy: Conf Ser 1850 (2021) 012102.
[21] P. Tamizharasi, R. Vijayaragavan, A. Magesh, Heat and Mass transfer analysis of the peristaltic driven flow of nanofluid in an asymmetric channel, Partial. Diff. Eq. Appl. Math. 4 (2021) 100087.
[22] R. Vijayaragavan, P. Tamizharasi, A. Magesh, Brownian motion and thermoporesis effects of nanofluid flow through the peristaltic mechanism in a vertical channel, J. Por. Media. 25 (6) (2022) 65-81.
[23] A. Magesh, P. Tamizharasi, R. Vijayaragavan, MHD flow of (Al2O3/H2O) nanofluid under the peristaltic mechanism in an asymmetric channel, Heat. Trans. 51 (7) (2022) 6563-6577.
[24] H Sato, T. Kawai, T. Fujita, M. Okabe, Two-dimensional peristaltic flow in curved channels, Trans. Japan. Soc. Mech. Eng. B.66 (2000) 679–685.
[25] N. Ali, M. Sajid, T. Javed, Abbas, Non-Newtonian Fluid, Flow Induced by Peristaltic Waves in a Curved Channel, Eur. J. Mech. B/Fluids.29 (2010) 387-394.
[26] S. Noreen, T. Hayat, A. Alsaedi, Magneto hydrodynamic peristaltic flow of a pseudo plastic fluid in a curved channel, Z. Naturforschung. A. 29 (2010) 387–394.
[27] T. Hayat, M. Javed, A.A. Hendi, Peristaltic Transport of Viscous Fluid in a Curved Channel with Compliant Walls, Int. J. Heat. Mass. Trans. 54 (2010) 1615-1621.
[28] T. Hayat, S. Hina, A.A. Hendi, S. Asghar, Effect of Wall Properties on the Peristaltic Flow of a Third Grade Fluid in a Curved Channel with Heat and Mass Transfer, Int.J. Heat. Mass. Transf. 54 (2011) 5126-5136.
[29] T. Hayat, S. Noreen, A. Alsaedi, Effect of an induced magnetic field on peristaltic flow of non-Newtonian fluid in a curved channel, J. Mech. Med. Biol.12 (2012) 1250058–1250084.
[30] S. Hina, T. Hayat, A. Alsaedi, Heat and mass transfer effects on the peristaltic flow of Johnson–Segalman fluid in a curved channel with compliant walls, Int. J. Heat. Mass. Transf. 55 (2012) 3511–3521.
[31] N.S. Akbar, E.N. Maraj, Adil Wahid Butt, Copper nano particles impinging in a curved channel with complaint walls and peristalsis, Eur. Phys. J. Plus.129 (8) (2014) 183.
[32] N.S. Akbar, E.N. Maraj, S. Nadeem, Copper nano particle analysis for peristaltic flow in curved channel with heat transfer characteristics, Eur. Phys. J. Plus.129 (2014) 149.
[33] S. Nadeem, E.N. Maraj, N.S. Akbar, Investigation of peristaltic flow of Williamson nano fluid in a curved channel with compliant walls, Appl. Nanosci. 4 (2014) 511–521.
[34] N.S. Akbar, Adil Wahid Butt, Carbon Nano tubes analysis for the peristaltic flow in curved channel with heat transfer, Appl. Math. Comp.259 (2016) 231–241.
[35] K. Javid, N. Ali, M. Sajid, Simultaneous effects of viscoelasticity and curvature on peristaltic flow through a curved channel, Meccanica. 51 (2016) 87-98.
[36] N. Ali, K. Javid, M. Sajid, A. Zaman, T. Hayat, Numerical simulations of Oldroyd 8-constant fluid flow and heat transfer in a curved channel, Int. J. Heat. Mass. Transf. 94 (2016) 500–508.
[37] T. Hayat, H. Zahir, A. Tanveer, A. Alsaedi, Soret and Dufour effects on MHD peristaltic transport of Jeffrey fluid in a curved channel with convective boundary conditions, Plos One. 12 (2) (2017) e0164854.
[38] Magesh A, Kothandapani M. Heat and mass transfer analysis on non-Newtonian fluid motion driven by peristaltic pumping in an asymmetric curved channel. Eur Phys J Spec Top 2021; 230:1447-1464.
[39] A. Magesh, M. Kothandapani, Analysis of Heat and Mass Transfer on the Peristaltic Movement of Carreau Nanofluids, J. Mech. Med. Biol.22 (1) (2022) 2150068.
[40] A. Magesh, V. Pushparaj, S. Srinivas, P. Tamizharasi, Numerical investigations of activation energy on the peristaltic transport of Carreau nanofluid through a curved asymmetric channel, Phys. Fluids. 35 (2023) 10.